PAUL SCHERRER INSTITUT

Paul Scherrer Institute
Pierre-André Duperrex

On-line calibration schemes for RF-based beam diagnostics

HB2012 Beijing, 17-20 Sept. 2012

Motivation

Some difficulties related to RF signal measurements:

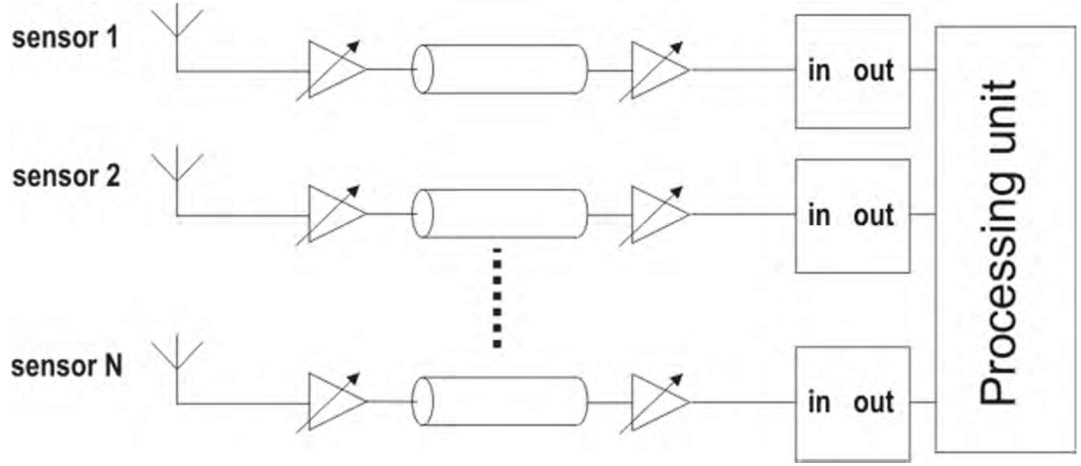

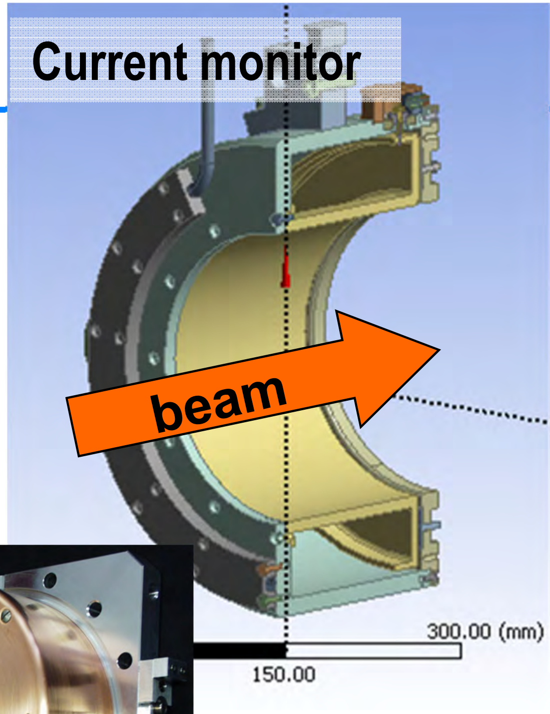

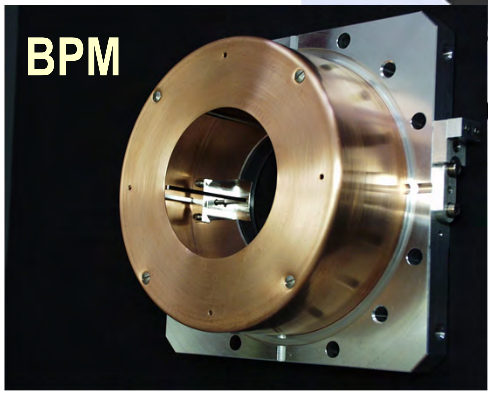

- Sensors 1 to N might have slightly different sensitivity.
- Difference in the overall gain between measurement chains introduces error.
- Temperature drifts may affect differently the electronic elements.
- Calibration may require some large effort, be time-consuming and possibly be required after repairs. Also repeated calibrations may be needed to confirm the gain.

⇨On-line calibration schemes may remove some of these difficulties.

First application:

on-line calibration scheme for beam current monitors

HIPA Beam Current Monitors

Measurement principles:
- coaxial resonator
- magnetic field directly proportional to the beam current
- tuned at 101.26MHz, the RF 2nd harmonic
- dimension: outer diameter: ~40cm, length: ~20cm

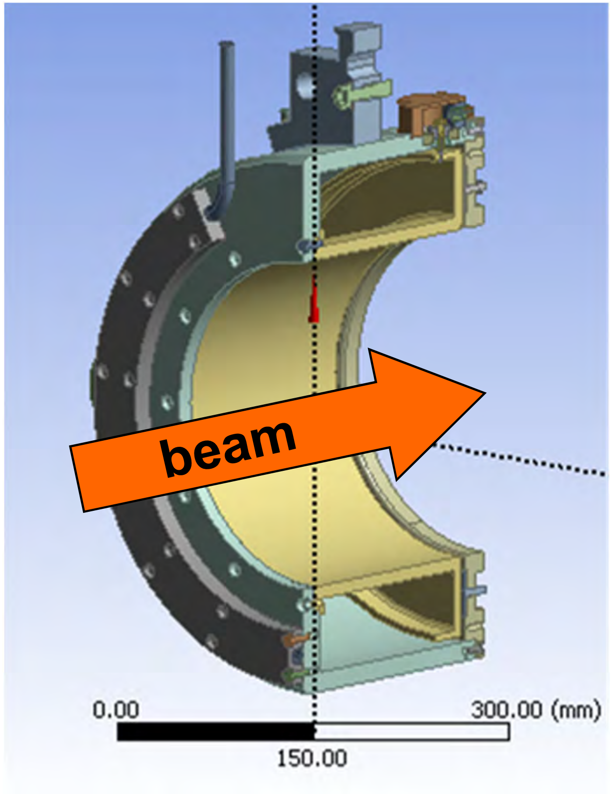

Advantages:
- simple design
- radiation resistant

Disadvantages:
- no absolute measurements
- temperature drifts

Challenge:

A beam current monitor (called MHC5) is in vacuum 8 m behind a 4cm graphite target.
This monitor is subject to a heat load due to scattered particles (~250W for a 2mA beam).
The resonator gain drift due to the heat load makes the beam current measurement challenging.

Resonance Condition

coaxial line with a capacitor shunt:

Coaxial line loss-less impedance with a shorted load: $Z_i = jZ_o \tan\left(\frac{2\pi f_m L}{c}\right)$

an inductive effect for: $\frac{2\pi f_m L}{c} < \frac{\pi}{2}$ *i.e.* $\frac{L}{\lambda_m} < \frac{1}{4}$

With the capacitor reactance: $X_c = \frac{1}{j2\pi f_m C}$

The parallel circuit is resonant when: $Z_i = -X_c$

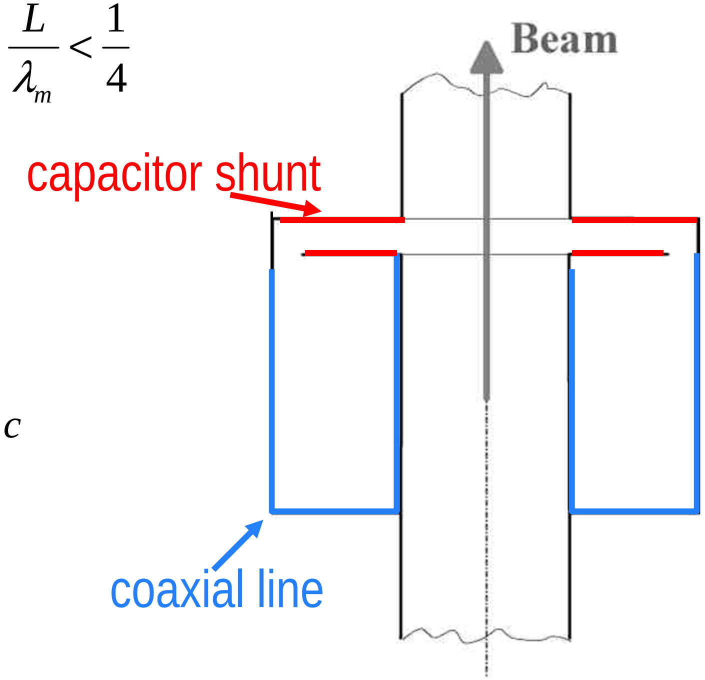

Resulting relation for resonance with a capacitor shunt:

L : *resonator length*
C : *capacitor shunt*
Z_o : *characteristic impedance*
λ_m : *resonant wavelength*

$$\boxed{\tan\left(\frac{2\pi L}{\lambda_m}\right) = \frac{\lambda_m}{2\pi c C Z_o}}$$

In our case: L ~ 15 cm

Universal Tuning Curve

- The "universal tuning curve" as relation between the resonator length and the required C value.

- The red line corresponds to the MHC5 conditions.

- Temperature drift will affect the length of the resonator, the shunt capacitance and the line impedance.

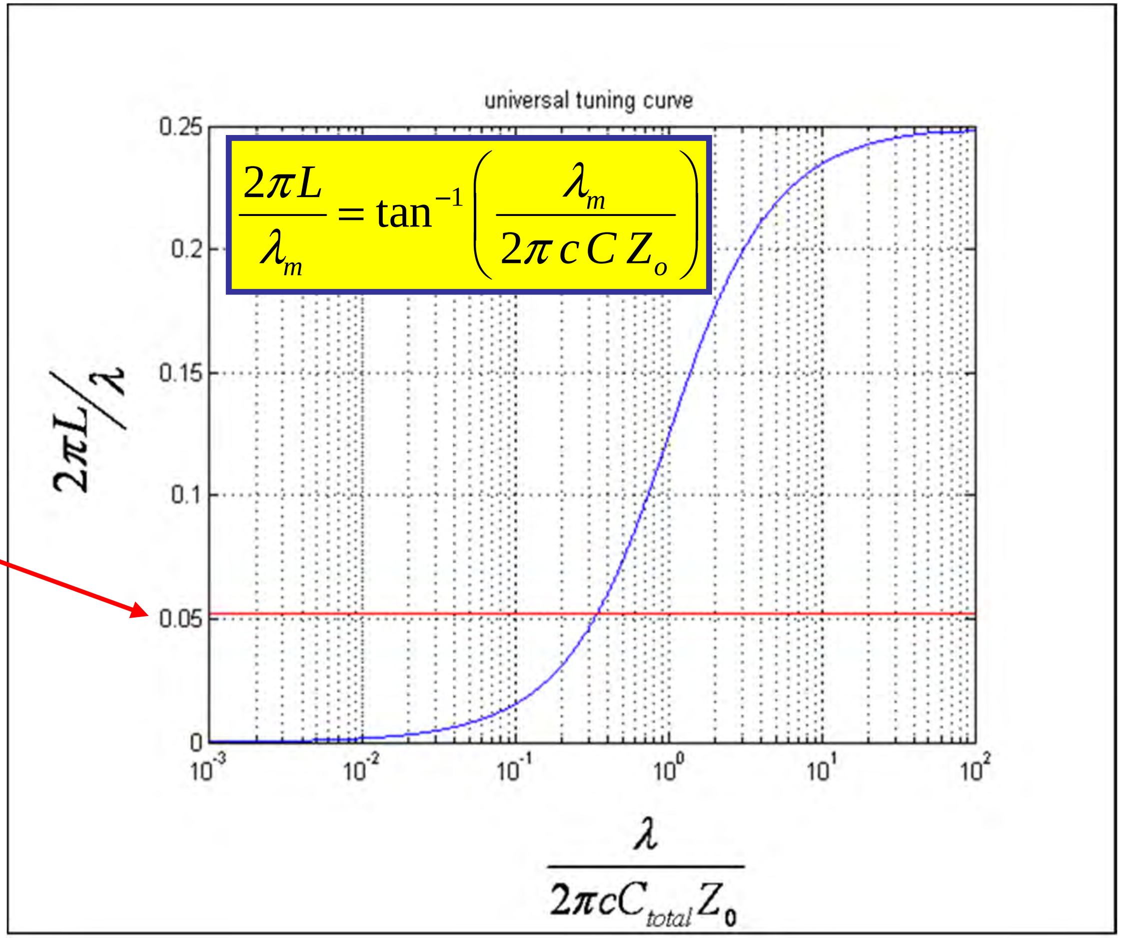

Temperature Effects

Optimization on the test bench to minimize the temperature drifts

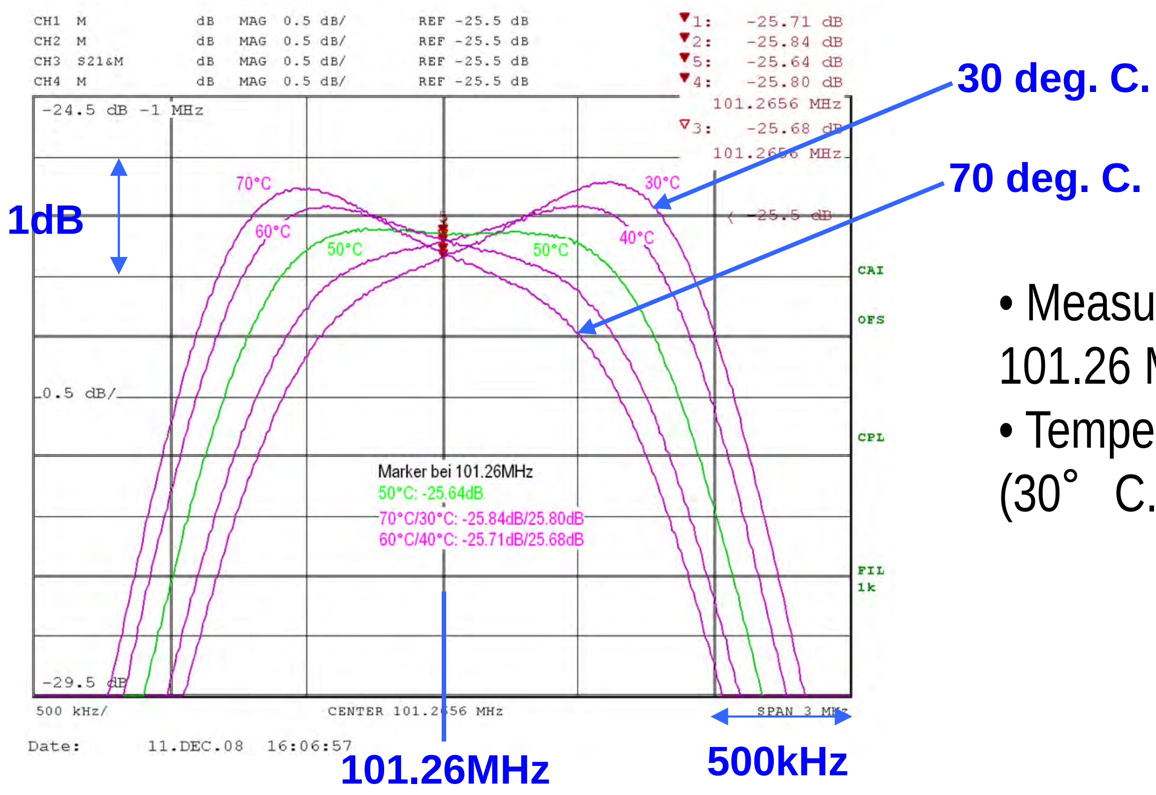

- Measurement of the transfer function around 101.26 MHz (2nd harmonic)
- Temperature coefficient: <0.01dB/° C (30° C..70° C) 0.3dB →3.5% in amplitude

But the drifts observed during operation are even larger, due to the non uniform temperature distribution.

MHC5 measured signal

measured: $S_m = K.S_{21}(2f_{RF}).I_{beam}$

$K : constant$

$S_{21}(2f_{RF}) : resonator\ gain\ at\ the\ RF\ 2nd\ harmonic$

$I_{beam} : beam\ current$

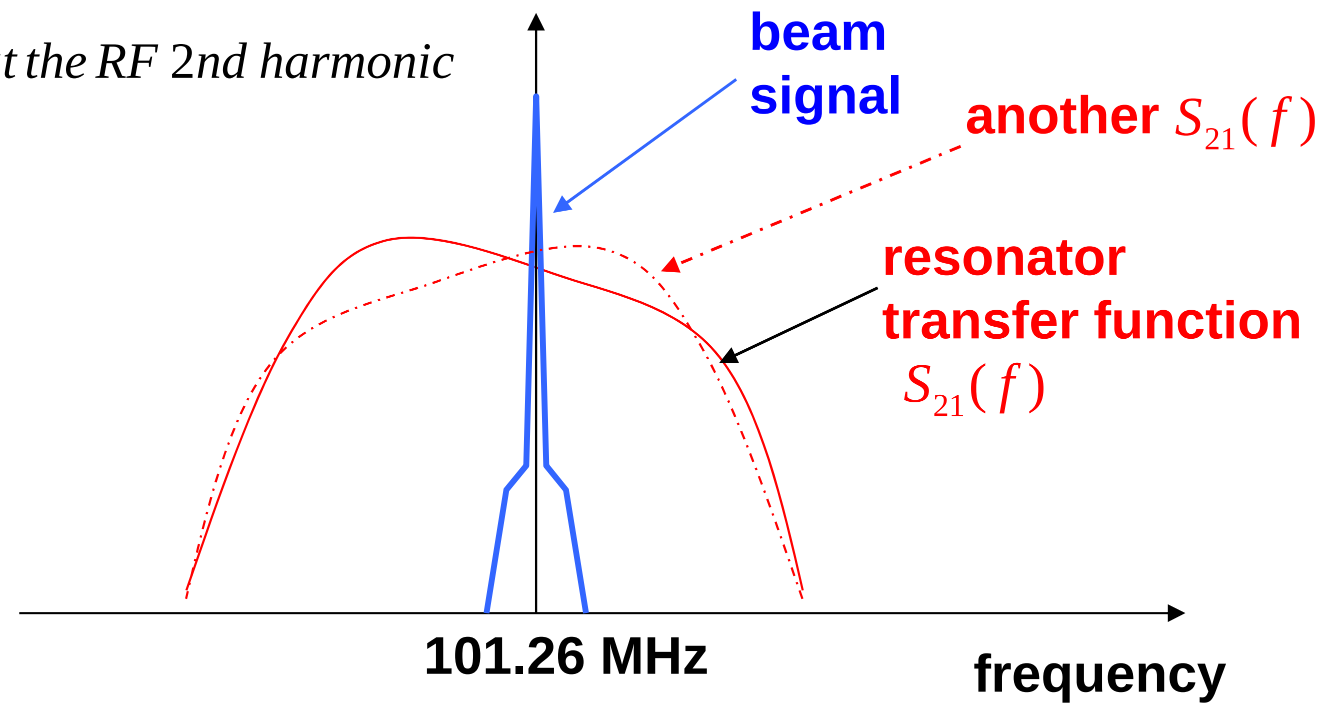

Change of the measured signal reflects either a change of beam current or a change of the resonator gain…or both…

Calibration Scheme Idea

$$S_m = K.S_{21}(2f_{RF}).I_{beam}$$

How to distinguish or to separate the two contributions?

Basic idea: measure some pilot signals at frequencies very close to the beam signal frequency (101.26MHz) to monitor the gain drift.

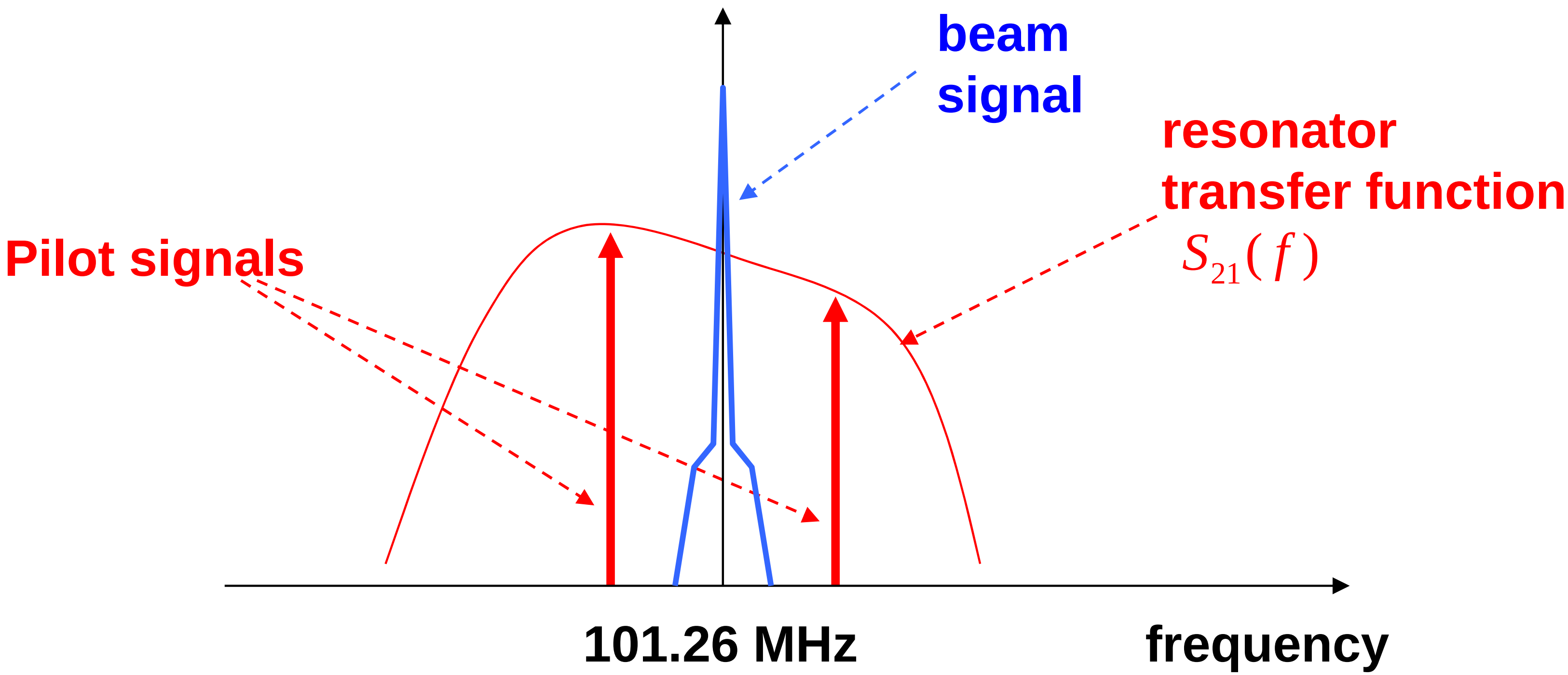

Calibration Scheme Idea

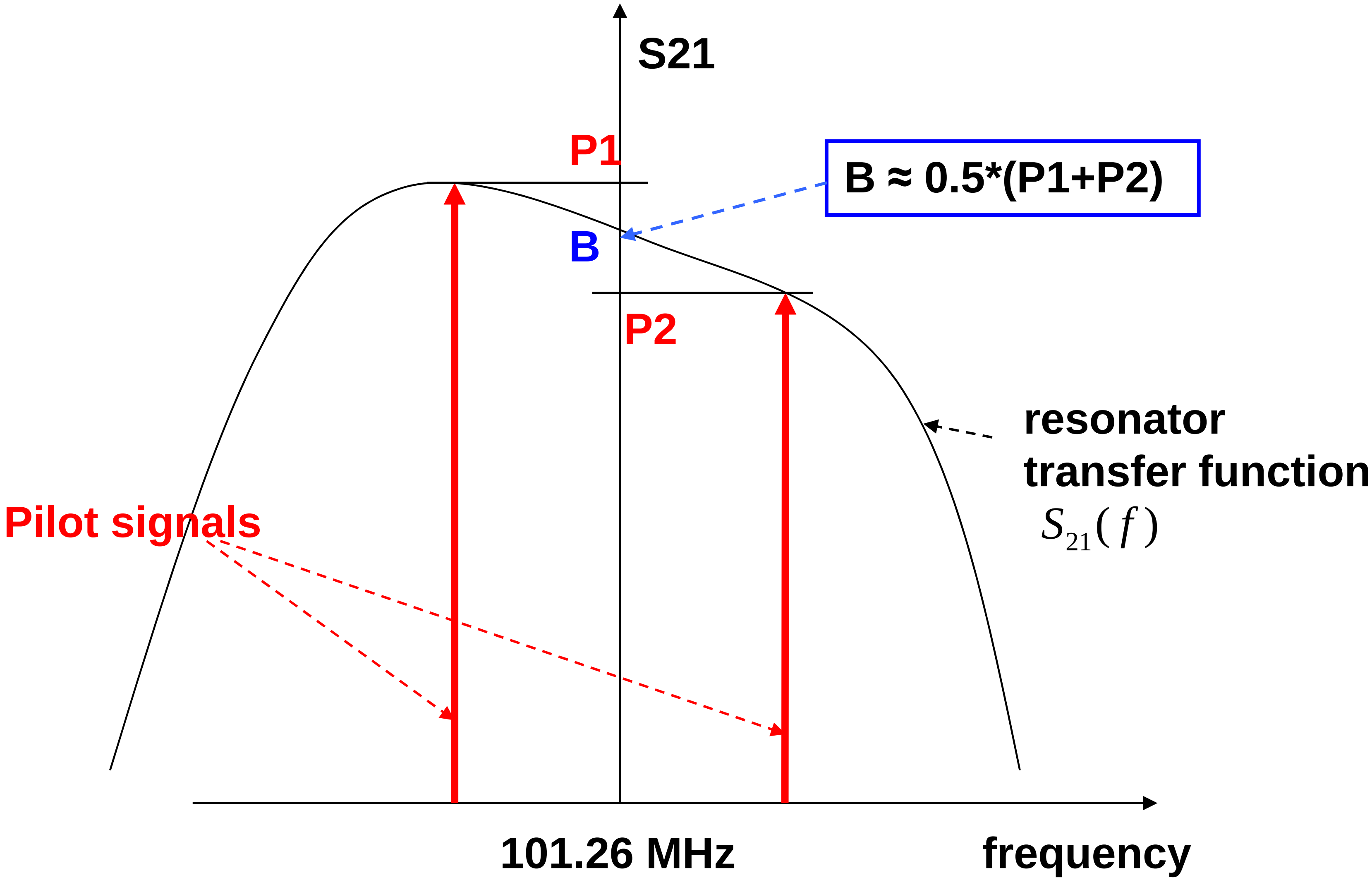

PAUL SCHERRER INSTITUT

Calibration Scheme Idea

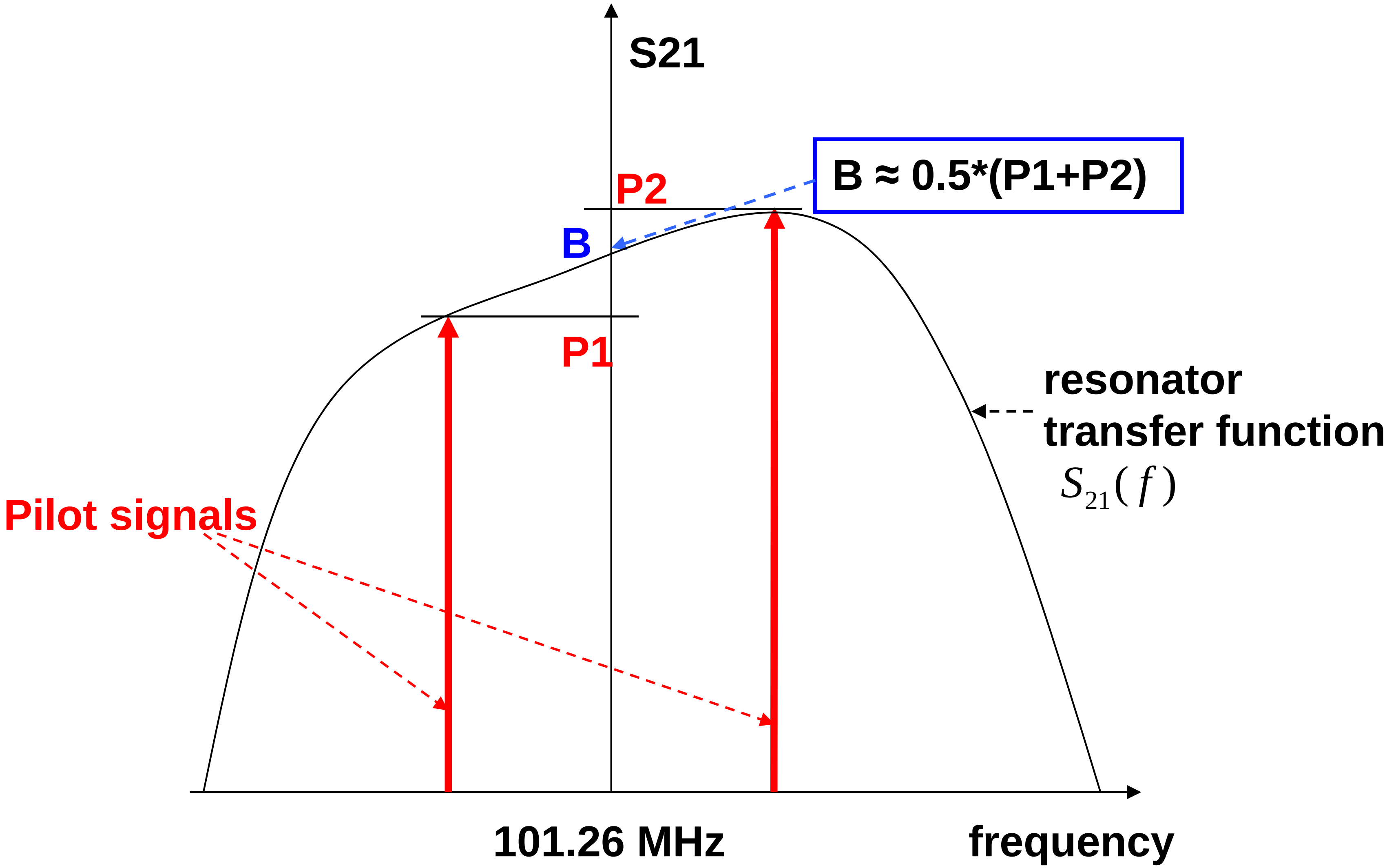

Calibration Concept

Implementation concept

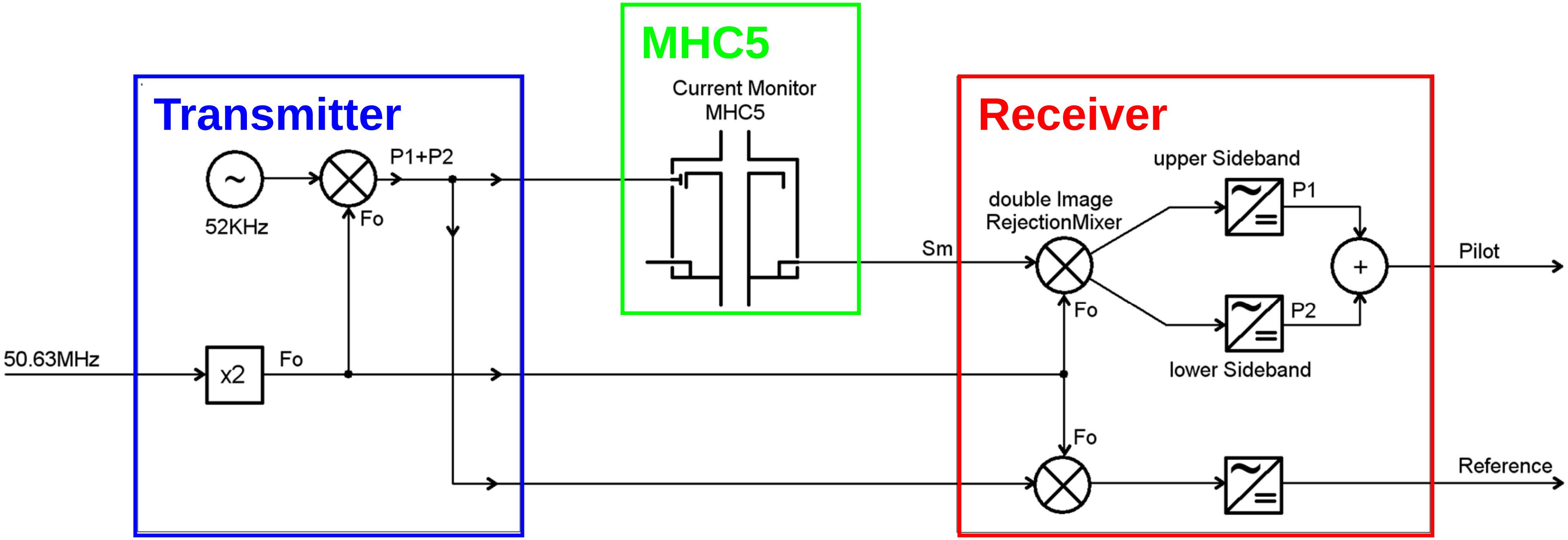

estimate of the resonator gain: $gain_{resonator} \; \alpha \; \frac{S_{Pilot}}{S_{Reference}}$

I/Q Demodulation & Image Rejection

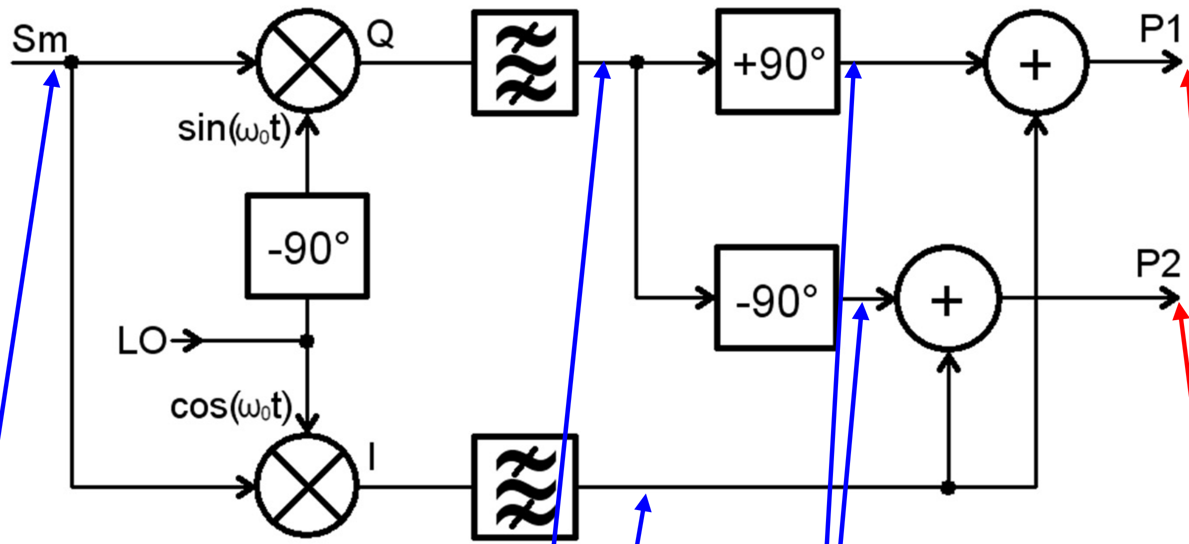

$$gain_{MHC5} \,\alpha\, \frac{P_1+P_2}{S_{Reference}}$$

$$S_m = P_{10}.\cos(\omega_1.t+\phi_1)+P_{20}.\cos(\omega_2.t+\phi_2)+S_{beam}.\cos(\omega_0.t)$$

$$S_Q(t) = \frac{1}{2}P_{10}.\sin(\Delta\omega.t-\phi_1)-\frac{1}{2}P_{20}.\sin(\Delta\omega.t+\phi_2)$$

$$\Delta\omega = |\omega_{1,2}-\omega_0|$$

$$S_I(t) = \frac{1}{2}P_{10}.\cos(\Delta\omega.t-\phi_1)+\frac{1}{2}P_{20}.\cos(\Delta\omega.t+\phi_2)$$

$$S_{Q+90\deg}(t) = \frac{1}{2}P_{10}.\cos(\Delta\omega.t-\phi_1)-\frac{1}{2}P_{20}.\cos(\Delta\omega.t+\phi_2)$$

$$S_{Q-90\deg}(t) = -\frac{1}{2}P_{10}.\cos(\Delta\omega.t-\phi_1)+\frac{1}{2}P_{20}.\cos(\Delta\omega.t+\phi_2)$$

$$S_I(t)+S_{Q-90\deg}(t) = P_{20}.\cos(\Delta\omega.t+\phi_2)$$

$$S_I(t)+S_{Q+90\deg}(t) = P_{10}.\cos(\Delta\omega.t-\phi_1)$$

Calibration: Off-line comparison

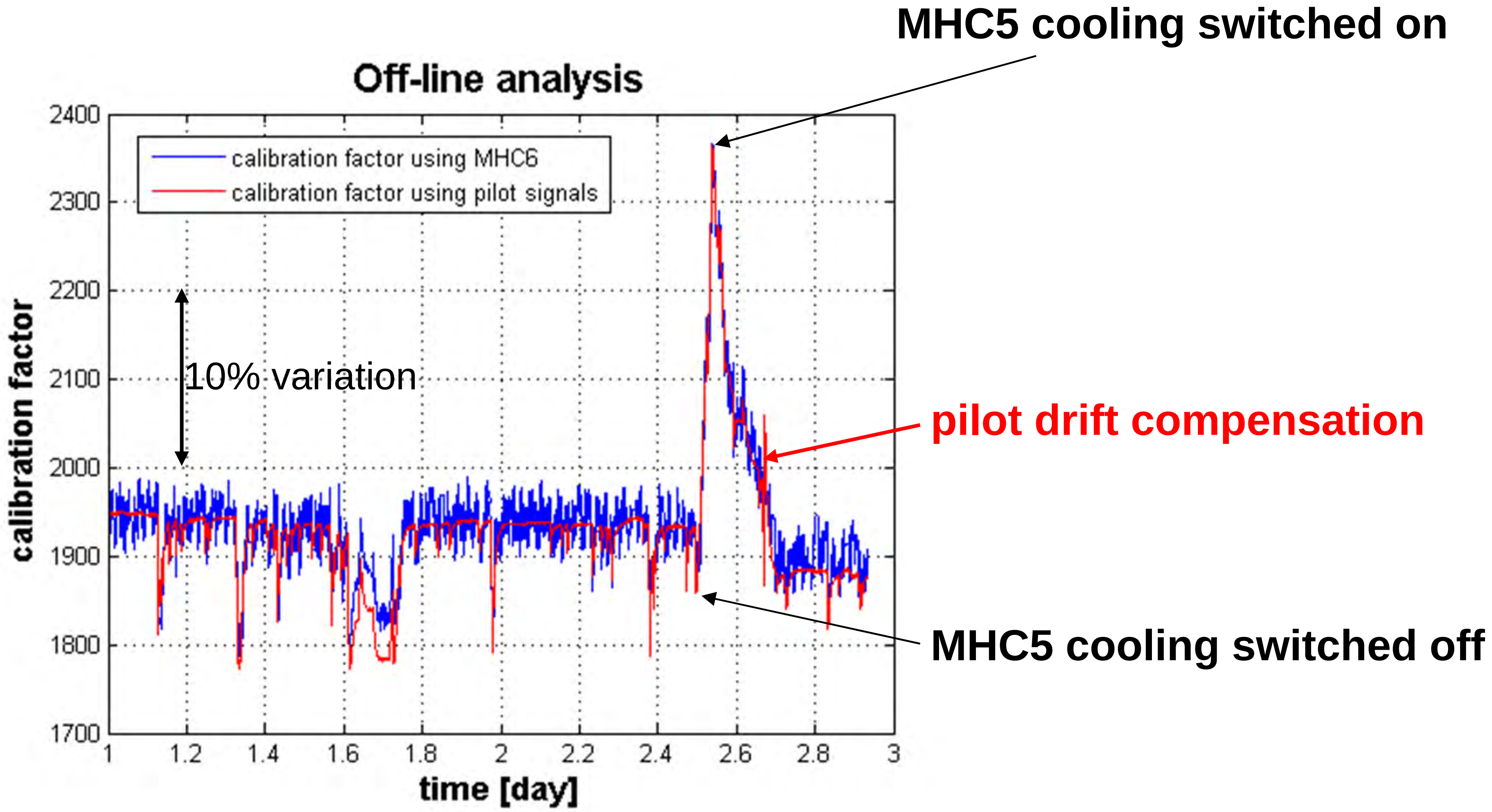

MHC6: another monitor on the same beam line, expected: $I_{MHC5} \cong I_{MHC6}$

⇨ **Possibility to use MHC6 for the MHC5 calibration**

The pilot drift compensation matches the calibration deduced from MHC6

Results during beam operation (2010)

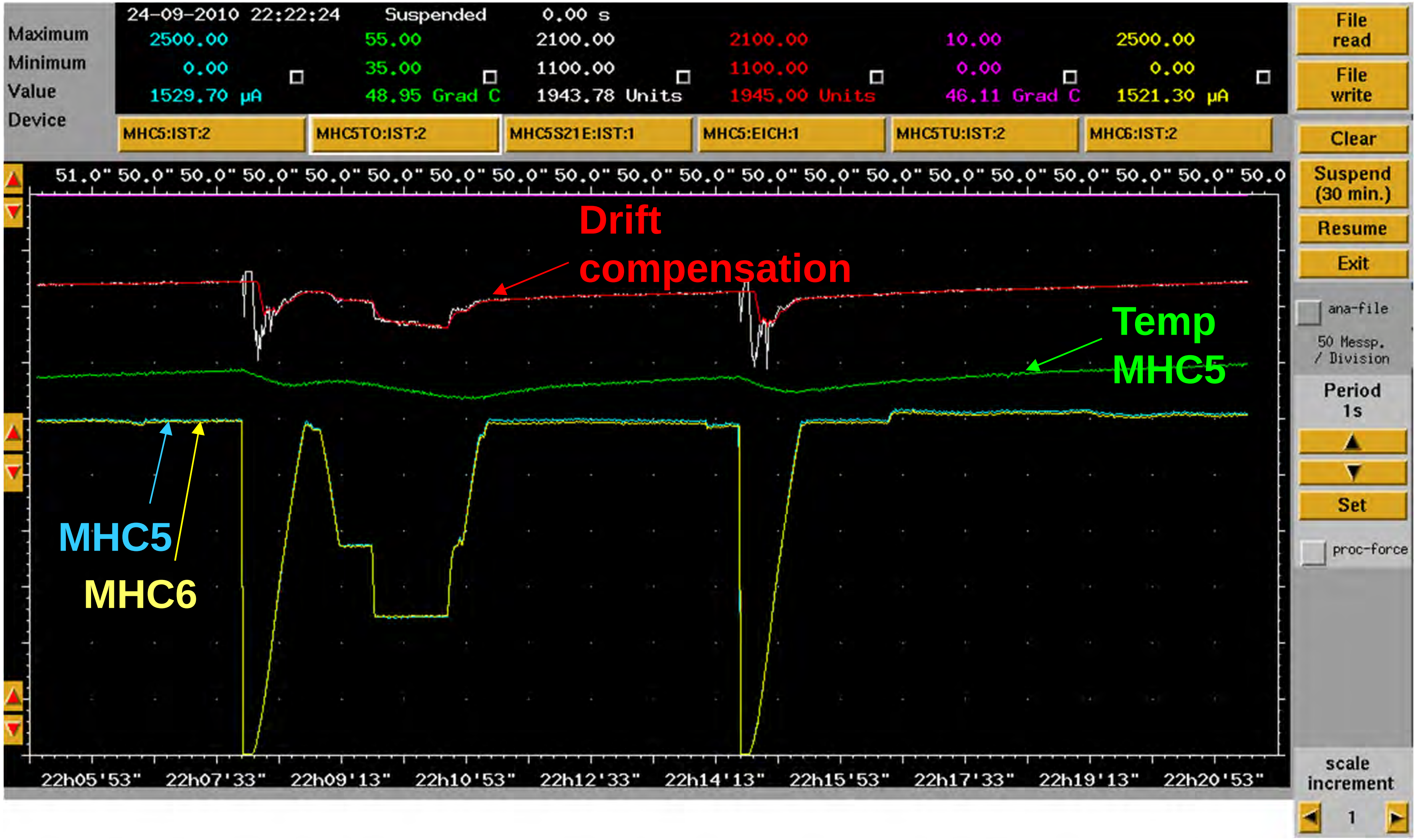

Initial Implementation

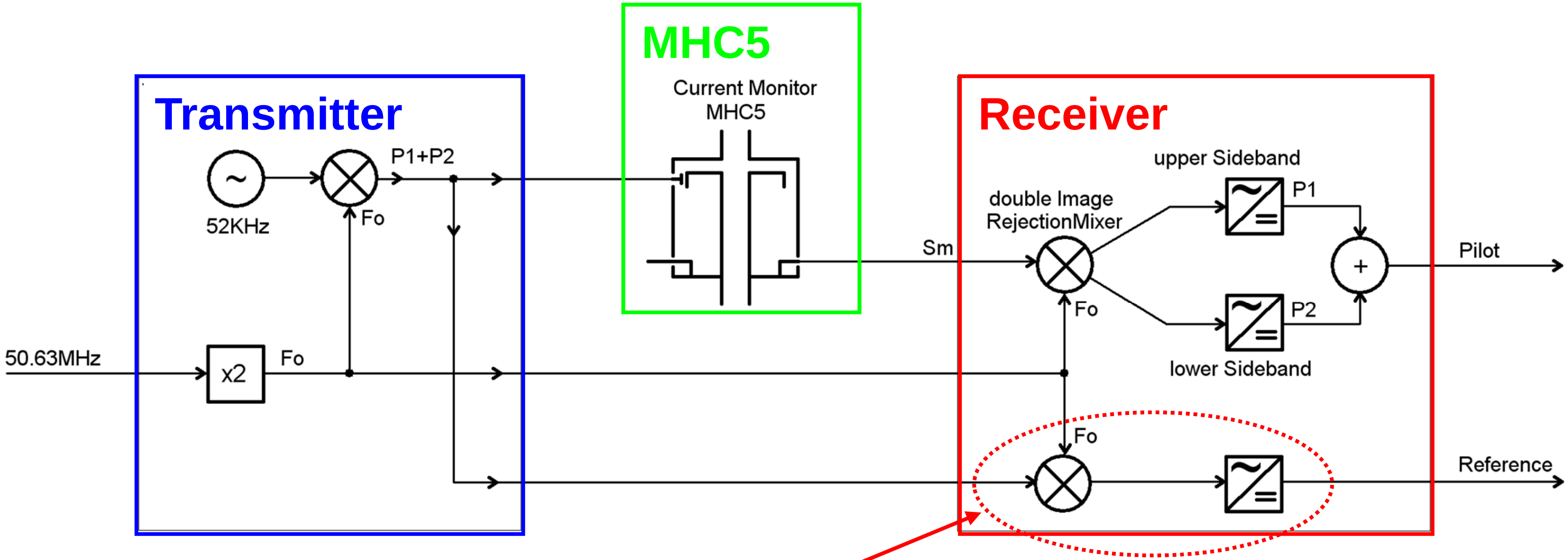

Phase drifts!

Improved Implementation

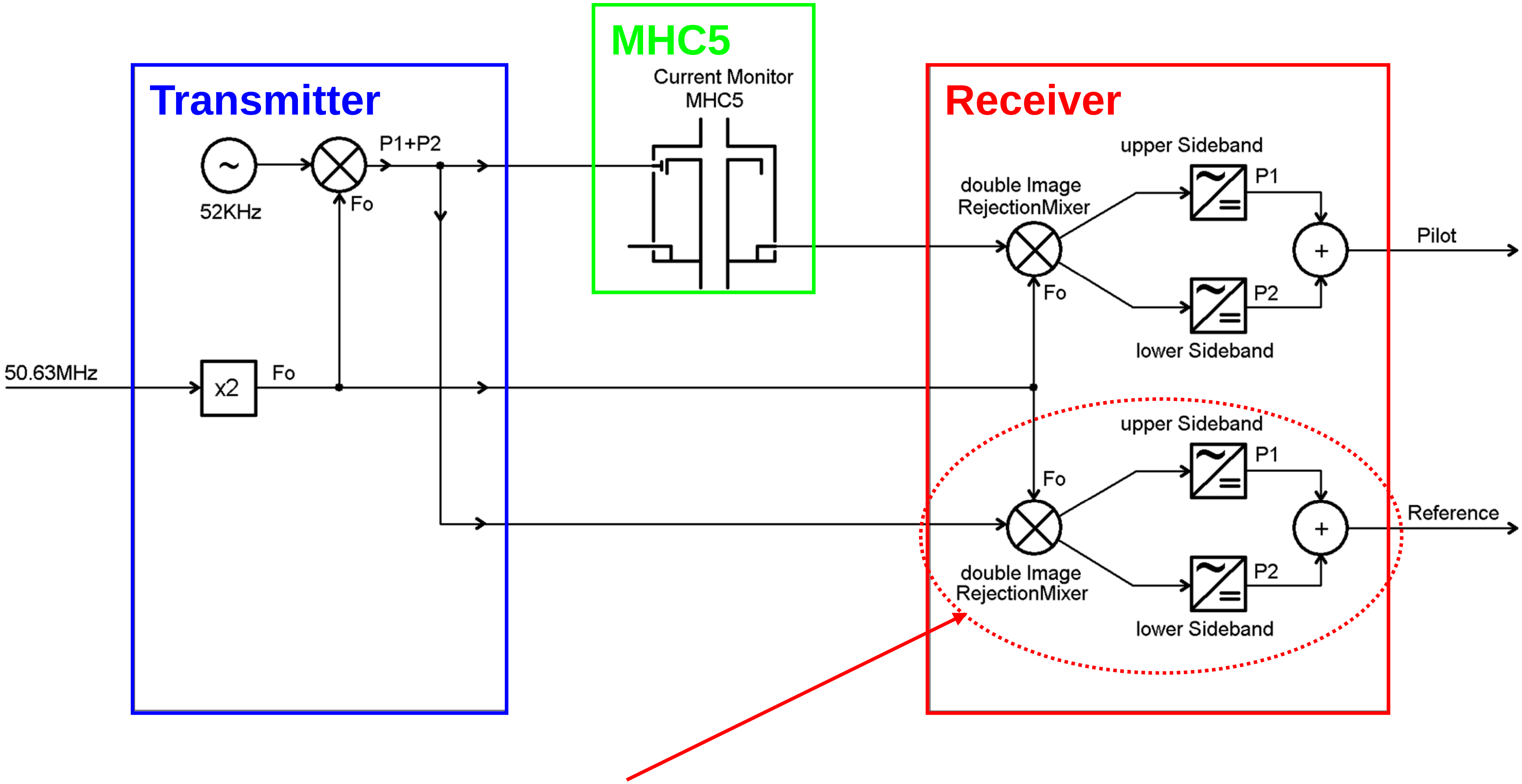

Upgrade: I/Q demodulation & image rejection for the reference too

2nd application:

on-line calibration scheme for beam position monitors

HIPA Beam Position Monitors

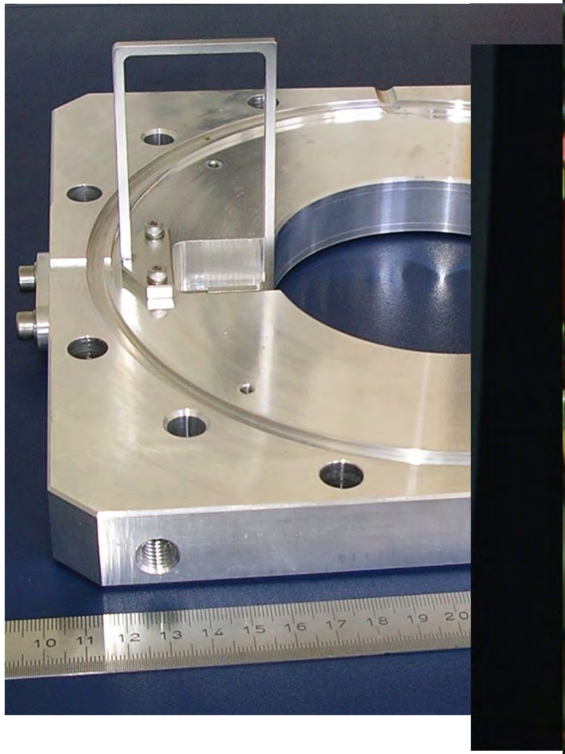

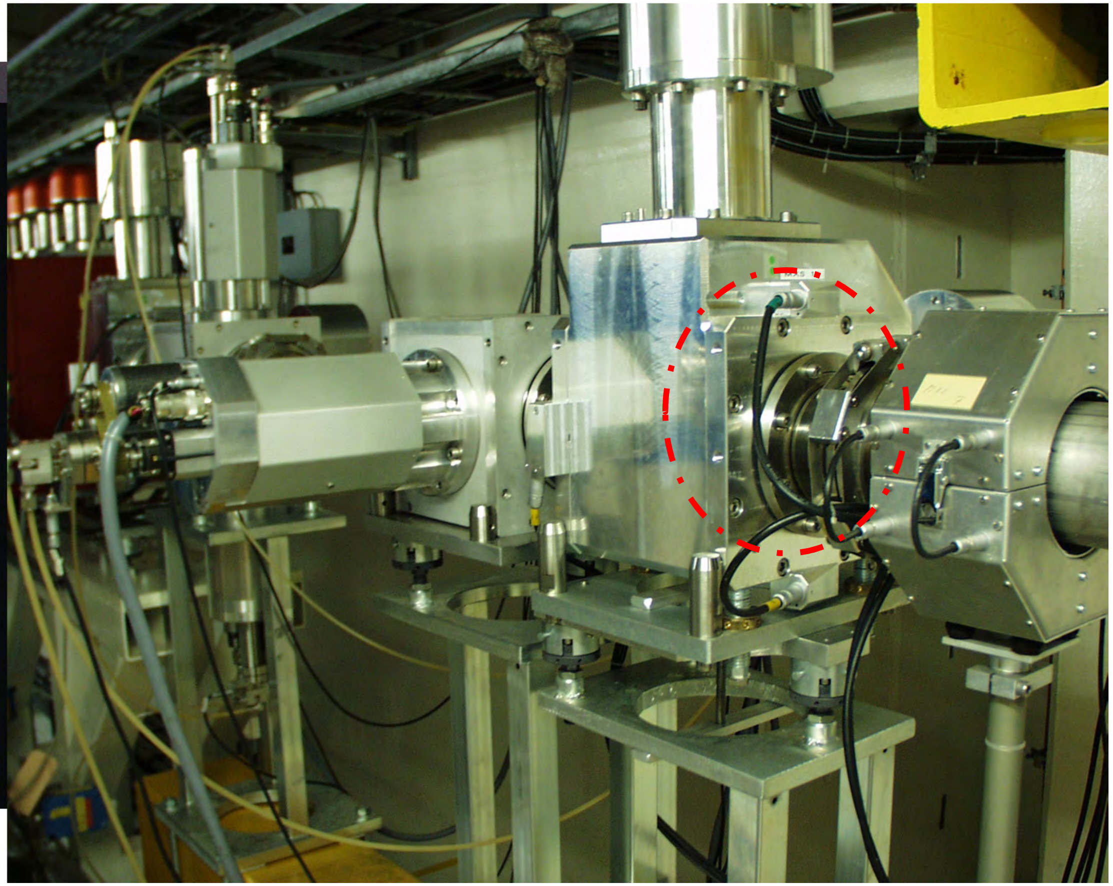

BPM probe

- magnetic pickup size: 4 x 8 cm
- x/y systems integrated with x/y profile monitors in a single box
- measurement of the RF 2nd harmonic (101.26MHz) signals

Position calculation based on the difference between the signal level of probes located on opposite side to the beam

$$\Delta x \; \alpha \; \frac{S^{+}_{beam} - S^{-}_{beam}}{S^{+}_{beam} + S^{-}_{beam}}$$

“standard” Implementation Overview

- based on digital receiver technology
- direct frequency down-converting of the RF 2nd harmonic (101.26MHz) signals (no analogue LO)

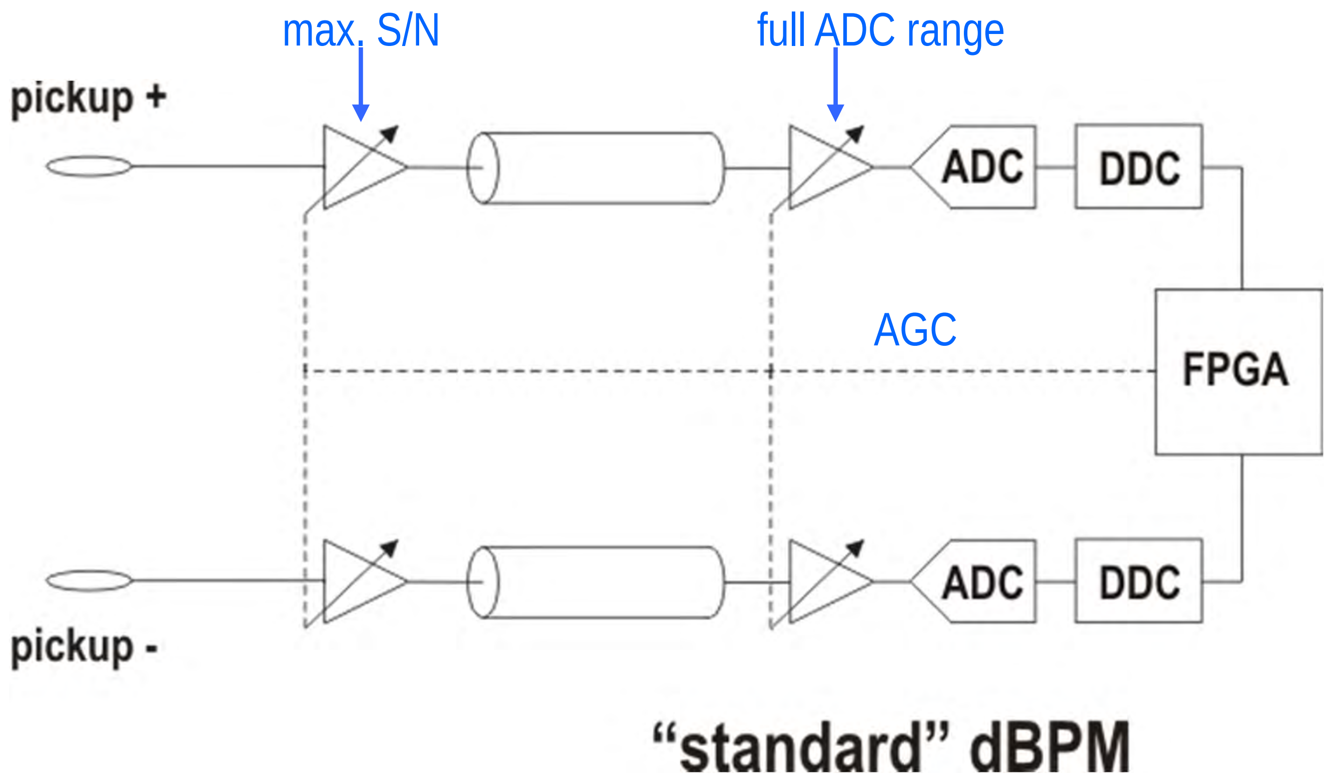

Issues related to absolute RF measurements

- requires tuning
- temperature drift may be a problem (electronics, cable attenuation)
- …

Implementation with Pilot Signals

- based on digital receiver technology
- direct frequency down-converting of the RF 2nd harmonic (101.26MHz) signals (no analogue LO)
- online measurement of individual channel overall gain using 101.18 MHz pilot signals

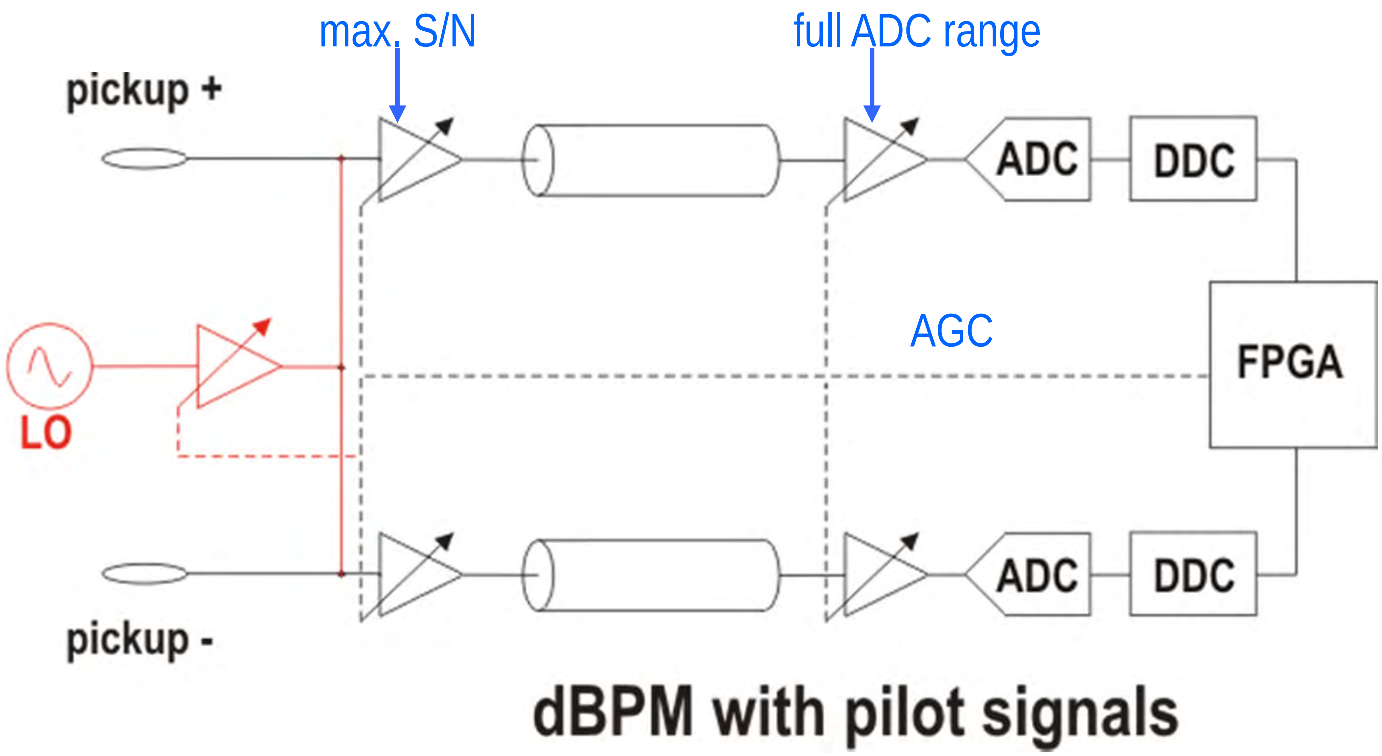

Using a pilot signal the whole measurement chain is calibrated.

dBPM electronics

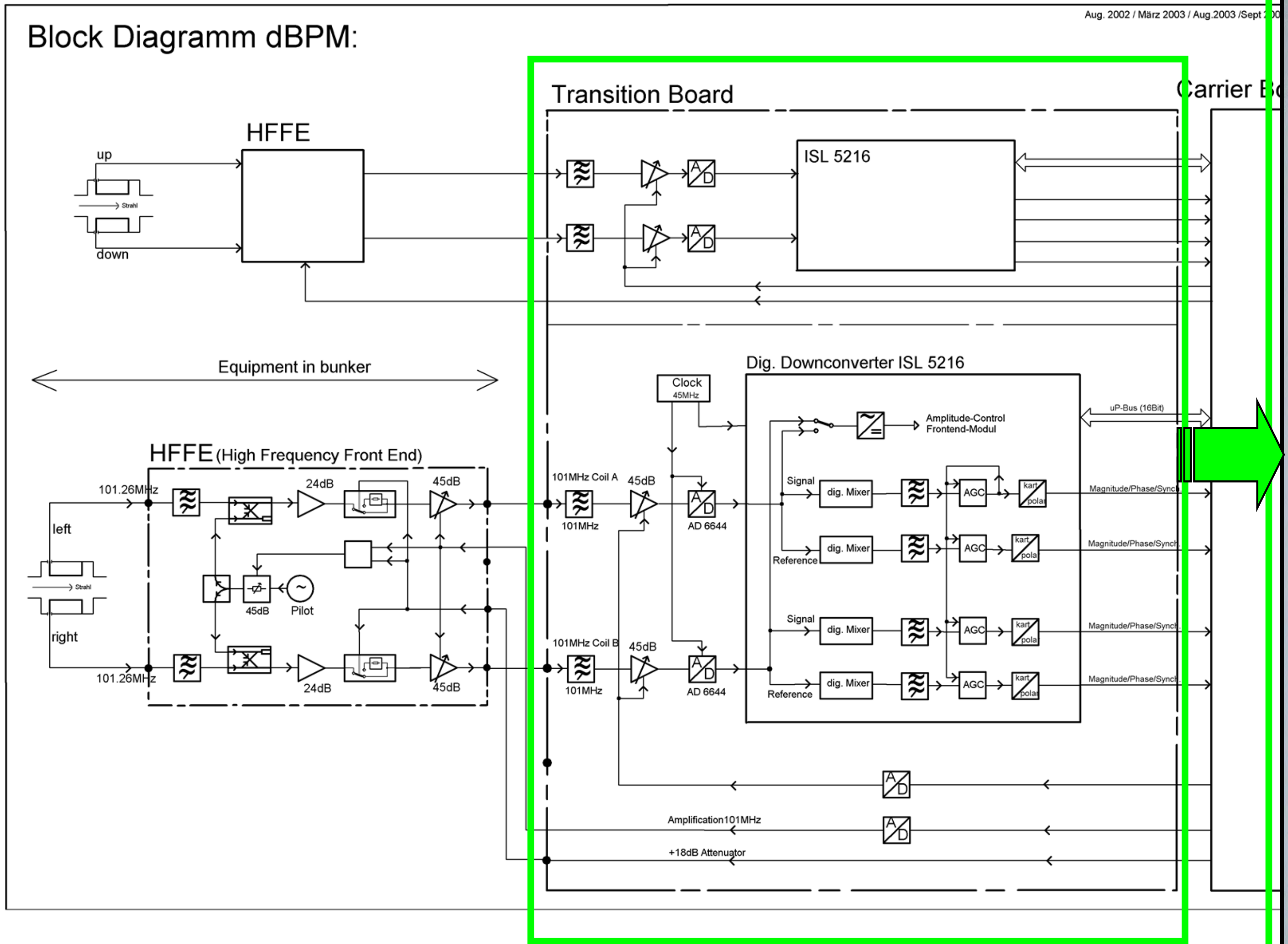

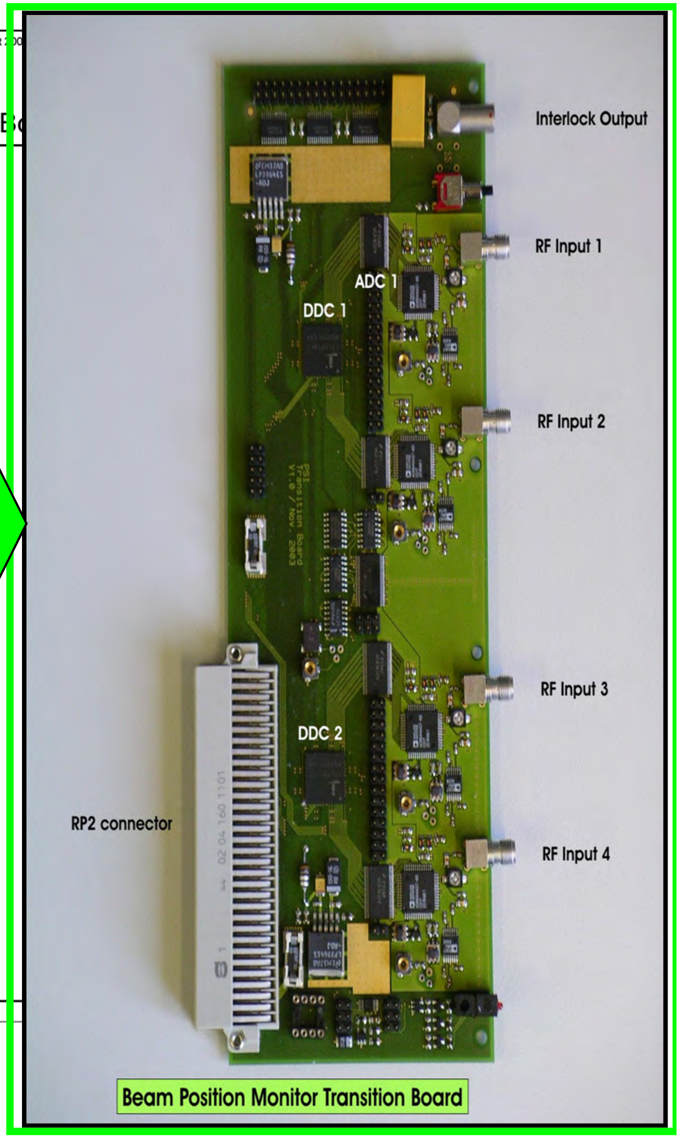

Position Calculation

including the pilot signals: $$\boxed{\Delta x \,\alpha\, \frac{S_n^{+} - S_n^{-}}{S_n^{+} + S_n^{-}}}$$

$$with \quad S_n^{+(-)} = \frac{S_{beam}^{+(-)}}{S_{pilot}^{+(-)}} \; normalized \;\, signal \;\, of \;\, sensor + or -$$

$$S_{beam}^{+(-)} : beam \; component \; of \;\, sensor + or -$$

$$S_{pilot}^{+(-)} : pilot \; signal \; of \;\, sensor + or -$$

Some concerns about the degradation of the signal-to-noise ratio (SNR)

Signal-to-Noise Ratio

Signals analyzed: raw, pilot and normalized signals from the right pickup of MXS3

S^{+}_{beam} $\sigma \approx 4\%$

S^{+}_{pilot} $\sigma \approx 4\%$

$$S^{+}_{n} = \frac{S^{+}_{beam}}{S^{+}_{pilot}}$$ $\sigma \approx 1\%$

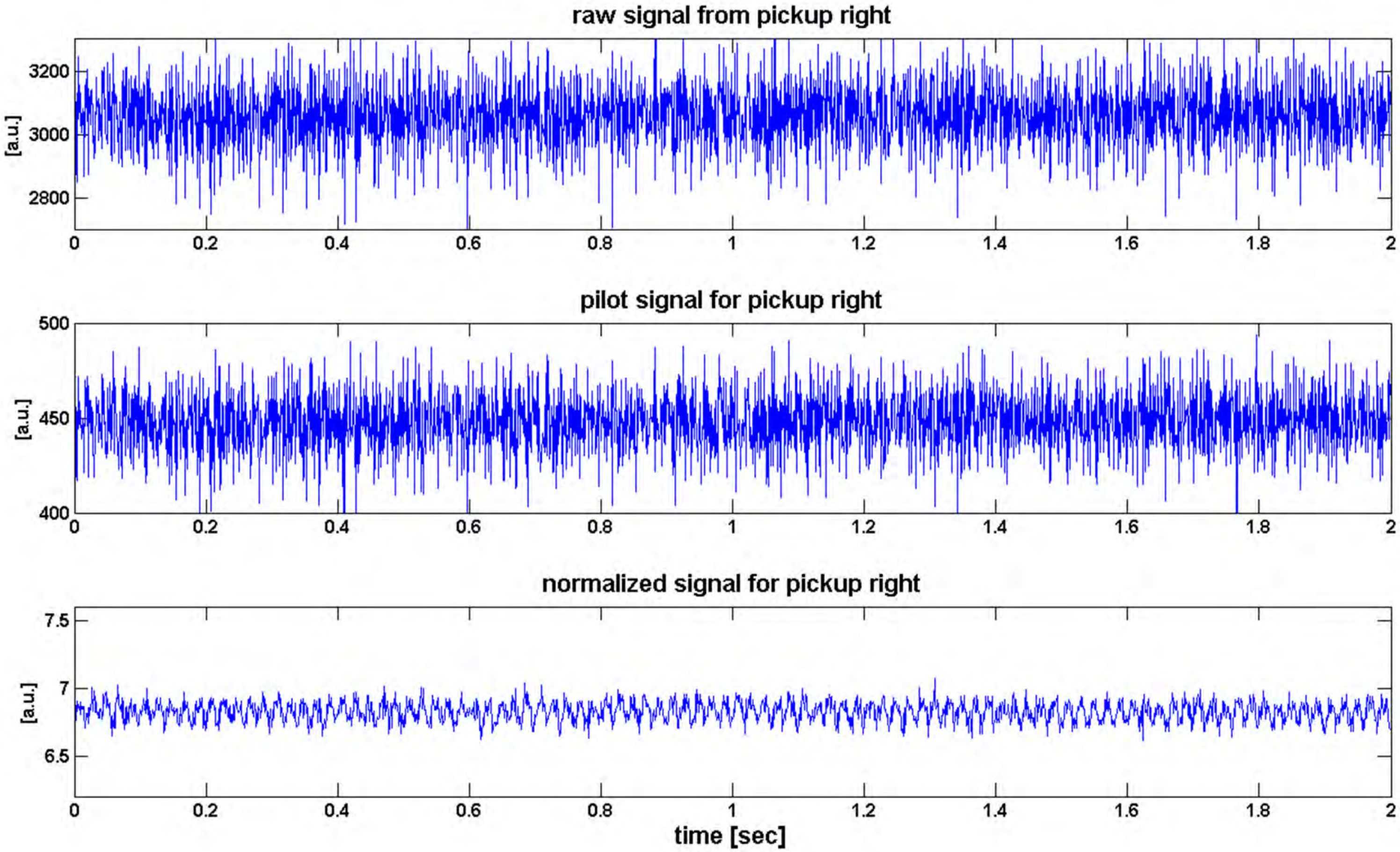

The relative standard deviation decreases by a factor 4 for the normalized signal!

SNR has improved for the normalized signal !

Correlation between Pilot and Beam Signals

Coherence Spectra for different beam, pilot and normalized signal combinations

$$C_{xy}(f) = \frac{\left|P_{xy}(f)\right|^2}{P_{xx}(f)P_{yy}(f)}$$

The Welch method using a Hanning window and 50% overlap has been applied.

Measurement conditions

- 1.97mA beam current
- BPM MXS3 & MXS4

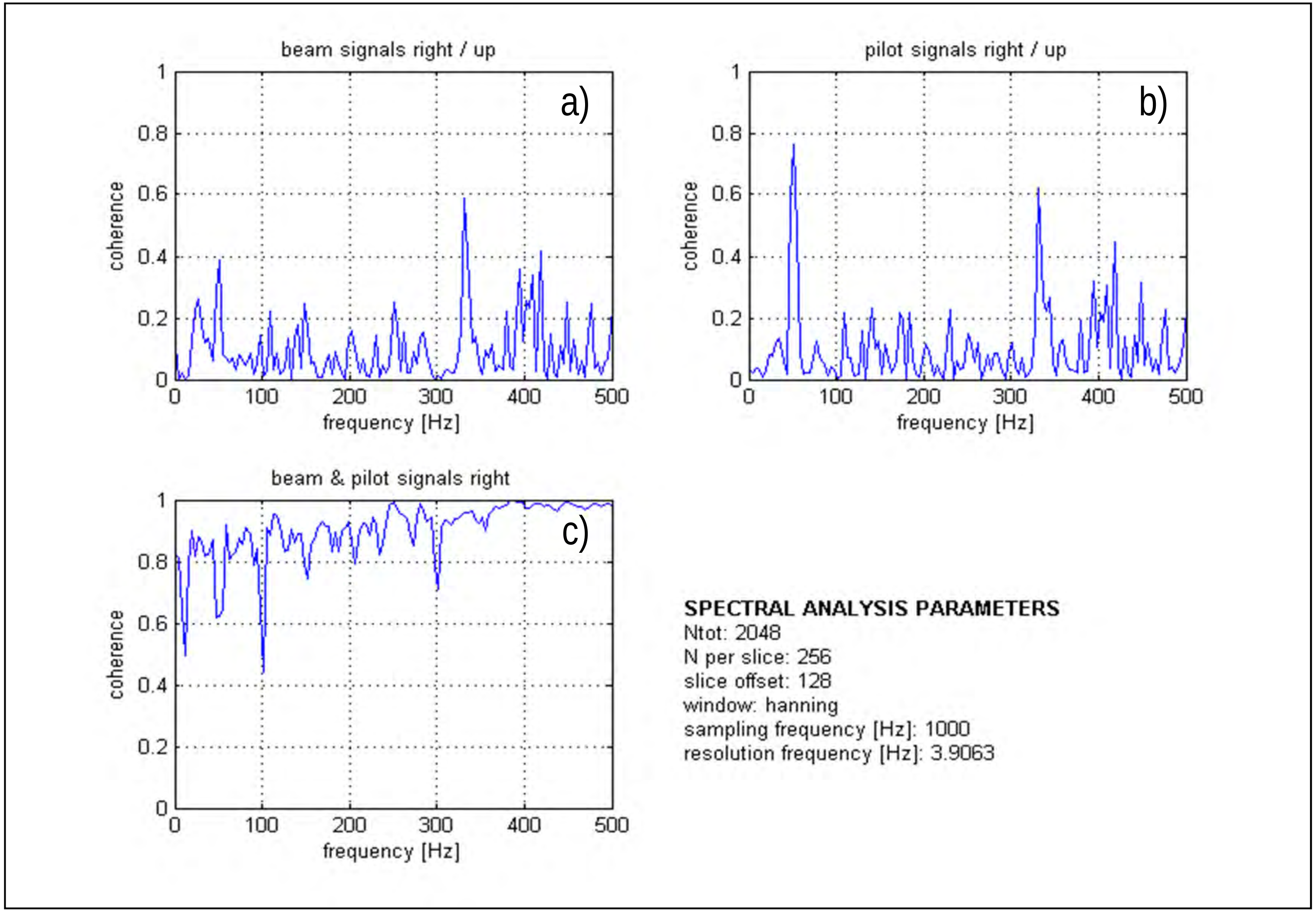

Correlation between Pilot and Beam Signals

Coherence Spectra for different beam, pilot and normalized signal combinations

$$C_{xy}(f) = \frac{\left|P_{xy}(f)\right|^2}{P_{xx}(f)P_{yy}(f)}$$

The Welch method using a Hanning window and 50% overlap has been applied.

Measurement conditions

- 1.97mA beam current
- BPM MXS3 & MXS4

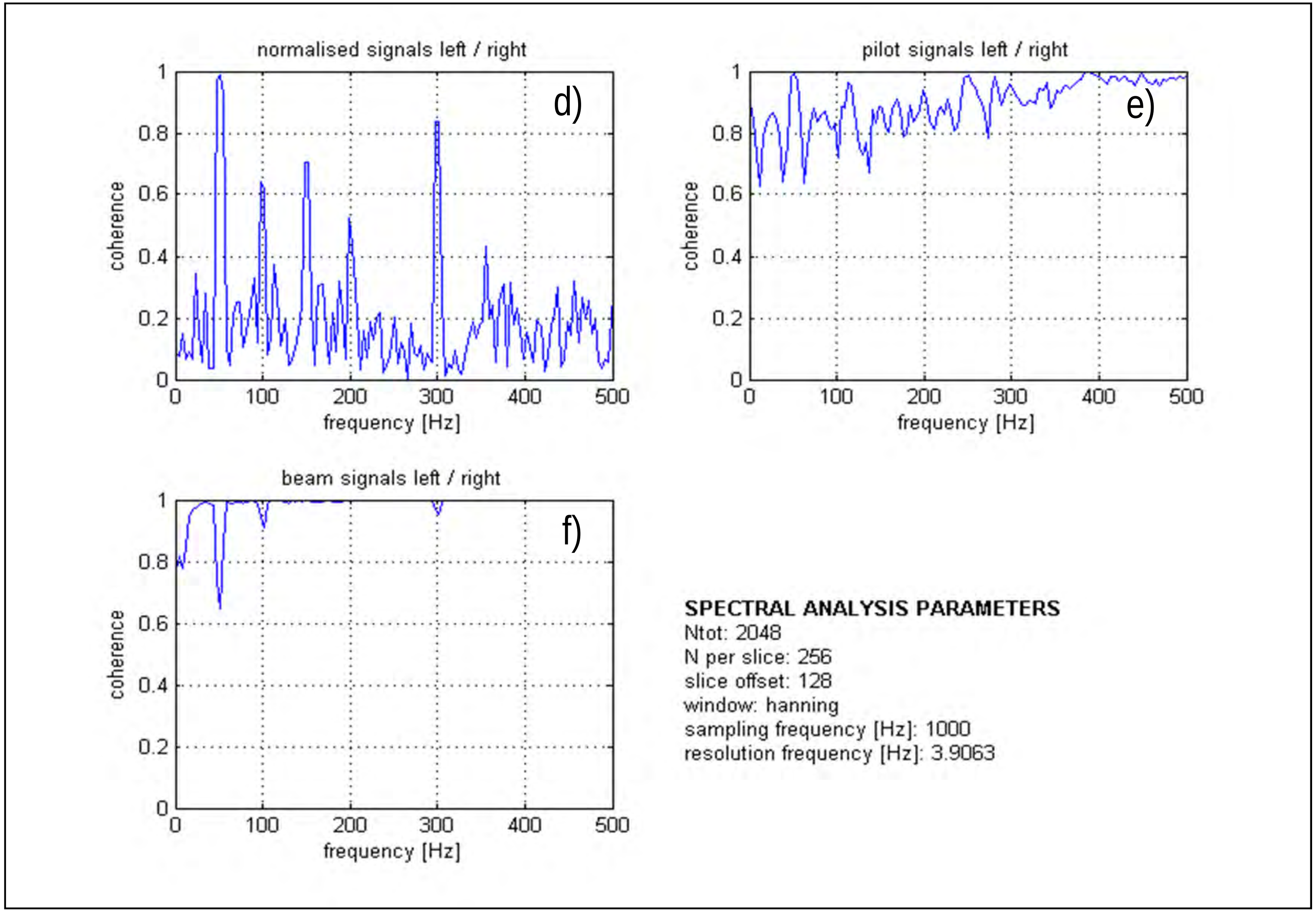

Correlation between Pilot and Beam Signals

Coherence Spectra for different beam, pilot and normalized signal combinations

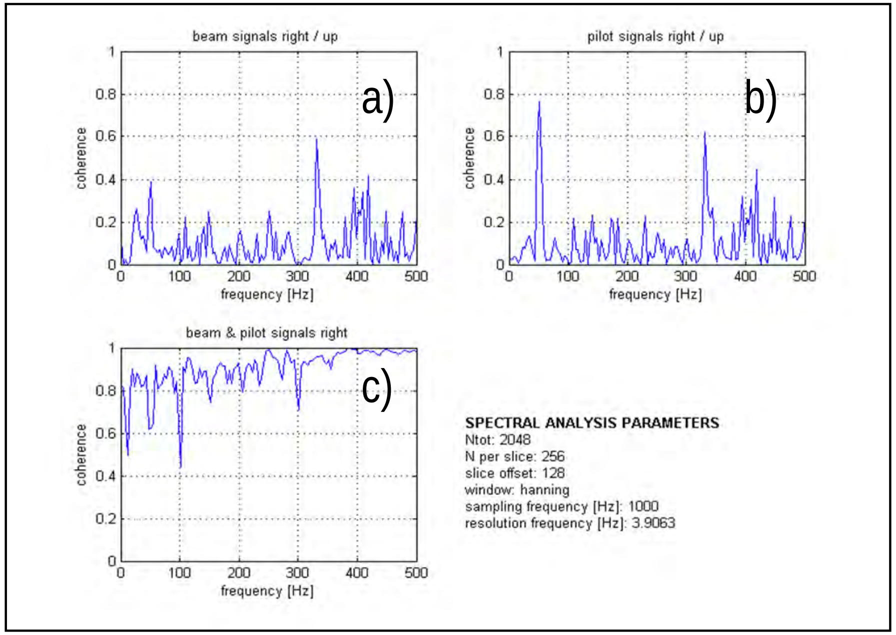

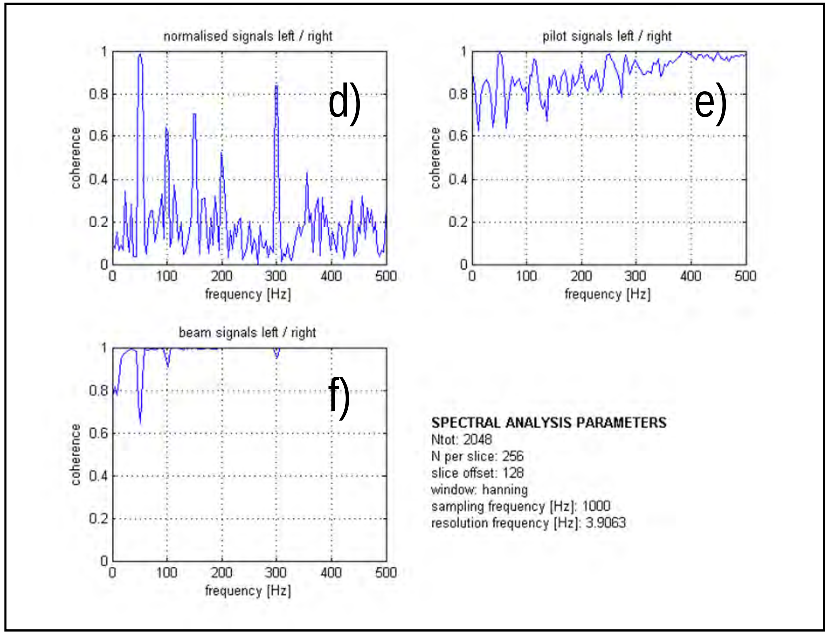

Observations

- horizontal and vertical signals are not correlated (a,b)
- beam signal and pilot signal noise highly correlated in the horizontal or vertical direction (c,e,f)
  - → mainly dominated by instrumental broadband noise
- normalized signals (d): only the 50Hz harmonics are correlated, real origin possible

- **Because pilot and beam signals are well correlated, the normalization improves the SNR !**

Pilot Scheme as (adaptive) Interference Cancelling

The dBPM pilot scheme can be seen as interference canceling system. This idea could be possibly further develop so to have an adaptive interference cancelling system.

Reminder: an IEEE 1975 paper from B. Widrow and al.

tuations in the atmosphere" (in Russian), *Izv. Vysch. Ucheb. Zaved., Radiofiz.*, vol. 17, pp. 105-112, 1974.

Section VII

[181] D. Fried, "Differential angle of arrival; theory, evaluation, and measurement feasibility," *Radio Sci.*, vol. 10, pp. 71-76, Jan. 1975.
[182] J. Lowry, J. Wolf, and J. Carter, "Acquisition and tracking assembly," McDonnell Douglas Tech. Rep. for Air Force Avionics Lab., Tech. Rep. AFAL-TR-73-380, Feb. 15, 1974.
[183] V. Lukin, V. Pokasov, and S. Khmelevstov, "Investigation of the time characteristics of fluctuations of the phases of optical waves propagating in the bottom layer of the atmosphere," *Radiophys. Quantum Electron.*, vol. 15, pp. 1426-1430, Dec. 1972.
[184] R. Lutomirski and R. Buser, "Phase difference and angle-of-arrival fluctuations in tracking a moving point source," *Appl. Opt.*, vol. 13, pp. 2869-2873, Dec. 1974.
[185] R. Lutomirski and R. Warren, "Atmospheric distortions in a retroreflected laser signal," *Appl. Opt.*, vol. 14, pp. 840-846, Apr. 1975.
[186] R. Lutomirski and H. Yura, "Imaging of extended objects through a turbulent atmosphere," *Appl. Opt.*, vol. 13, pp. 431-437, Feb. 1974.
[187] J. Pearson *et al.*, "Atmospheric turbulence compensation using coherent optical adaptive techniques," presented at OSA Topical Meeting on Propagation Through Turbulence, Boulder, Colo., paper ThB5-1, July 1974.
[188] D. Slepian, "Linear least-squares filtering of distorted images," *J. Opt. Soc. Amer.*, vol. 57, pp. 918-922, July 1967.
[189] H. Yura, Holography in a random spatially inhomogeneous medium," *Appl. Opt.*, vol. 12, pp. 1188-1192, June 1973.

Section VIII

[190] C. Gardner and M. Plonus, "The effects of atmospheric turbulence on the propagation of pulsed laser beams," *Radio Sci.*, vol. 10, pp. 129-137, Jan. 1975.

Section IX

[191] L. Apresyan, "The radiative-transfer equation with allowance for longitudinal waves," *Radiophys. Quantum Electron.*, vol. 16, pp. 348-356, Mar. 1973.
[192] Y. Barabanenkov, A. Vinogradov, Y. Kravtsov, and V. Tatarski, "Application of the theory of multiple scattering of waves to the derivation of the radiation transfer equation for a statistically inhomogeneous medium," *Radiophys. Quantum Electron.*, vol. 15, pp. 1420-1425, Dec. 1972.
[193] C. Martens and N. Jen, "Electromagnetic wave scattering from a turbulent plasma," *Radio Sci.*, vol. 10, pp. 221-228, Feb. 1975.
[194] I. Besieris, "Long-range electromagnetic random wave propagation using the parabolic equation method," *Dig. 1975 URSI Meet.*, p. 15, June 1975.

Adaptive Noise Cancelling: Principles and Applications

BERNARD WIDROW, SENIOR MEMBER, IEEE, JOHN R. GLOVER, JR., MEMBER, IEEE, JOHN M. McCOOL, SENIOR MEMBER, IEEE, JOHN KAUNITZ, MEMBER, IEEE, CHARLES S. WILLIAMS, STUDENT MEMBER, IEEE, ROBERT H. HEARN, JAMES R. ZEIDLER, EUGENE DONG, JR., AND ROBERT C. GOODLIN

Abstract—This paper describes the concept of adaptive noise cancelling, an alternative method of estimating signals corrupted by additive noise or interference. The method uses a "primary" input containing the corrupted signal and a "reference" input containing noise correlated in some unknown way with the primary noise. The reference input is adaptively filtered and subtracted from the primary input to obtain the signal estimate. Adaptive filtering before subtraction allows the treatment of inputs that are deterministic or stochastic, stationary or time variable. Wiener solutions are developed to describe asymptotic adaptive performance and output signal-to-noise ratio for stationary stochastic inputs, including single and multiple reference inputs. These solutions show that when the reference input is free of signal and certain other conditions are met noise in the primary input can be essentially eliminated without signal distortion. It is further shown that in treating periodic interference the adaptive noise canceller acts as a notch filter with narrow bandwidth, infinite null, and the capability of tracking the exact frequency of the interference; in this case the canceller behaves as a linear, time-invariant system, with the adaptive filter converging on a dynamic rather than a static solution. Experimental results are presented that illustrate the usefulness of the adaptive noise cancelling technique in a variety of practical applications. These applications include the cancelling of various forms of periodic interference in electrocardiography, the cancelling of periodic interference in

1693

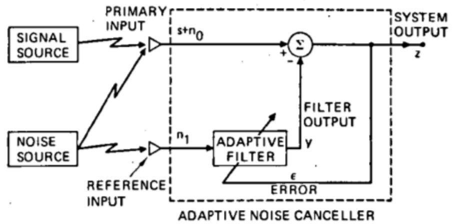

Fig. 1. The adaptive noise cancelling concept.

The first adaptive noise cancelling system at Stanford University was designed and built in 1965 by two students. Their

the concept

an application

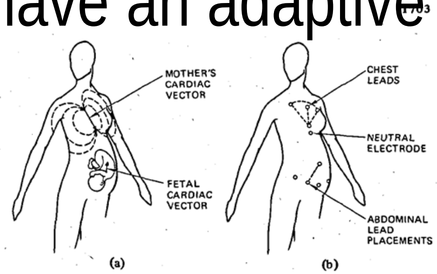

Fig. 14. Cancelling maternal heartbeat in fetal electrocardiography. (a) Cardiac electric field vectors of mother and fetus. (b) Placement of leads.

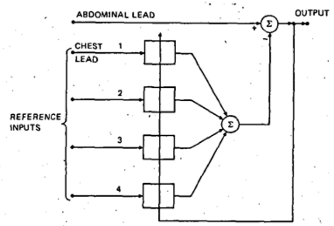

Fig. 15. Multiple-reference noise canceller used in fetal ECG experiment.

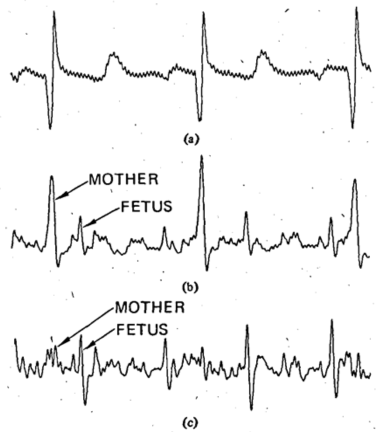

Fig. 16. Result of fetal ECG experiment (bandwidth, 3-35 Hz; sampling rate, 256 Hz). (a) Reference input (chest lead). (b) Primary input (abdominal lead). (c) Noise canceller output.

Summary

On-line calibration schemes:

- offer some clear accuracy improvements for sensors such as resonators affected by gain drifts due to temperature effects.
- do not require extensive calibration procedure
- may improve the signal-to-noise ratio (SNR) in some cases

Drawback: more elaborate instrumentation

Outlook: with the latest FPGA und electronic technology, more elaborate schemes may be implemented such as adaptive filtering or interference cancelling

PAUL SCHERRER INSTITUT

Thanks for your attention